# A Family of Binuclear Dysprosium(III) Radical Compounds with Magnetic Relaxation in ON and OFF States

Tian Han, Wei Shi,* Xiao-Ping Zhang, Lei-Lei Li, and Peng Cheng*

Department of Chemistry and Key Laboratory of Advanced Energy Materials Chemistry (MOE) and TKL of Metal and Molecule Based Material Chemistry, Nankai University, Tianjin 300071, People's Republic of China

Ⓢ *Supporting Information*

ABSTRACT: Four binuclear dysprosium compounds incorporating the radical ligand 2-(4-oxidopyridyl)-4,4,5,5-tetramethylimidazolin-1-oxyl-3-oxide (PyNONIT) have been successfully synthesized under appropriate conditions. Centrosymmetric bimetallic Dy_2O_2 cores in all of the compounds through double-μ_2-oxygen atoms of the *N*-oxide groups are realized in a metal−radical approach for the first time. Dimers **1** and **2**, of the same formula $\{[Dy(hfac)_3(PyNONIT)]_2\}_2$ (hfac = hexafluoroacetylacetonate) but obtained by different methods, which contain almost identical local symmetry of D_{4d} and Dy−(O)$_2$−Dy bridging fashion, however, display no out-of-phase alternating-current (ac) signal for **1** and slow relaxation of the magnetization for **2** corresponding to the difference of the crystal packing mode. The adduct $([Dy(hfac)_3(PyNONIT)]_2[Dy_{0.5}(hfac)_{1.5}(H_2O)]_2)$ (**3**) consists of two items, the dimer $[Dy(hfac)_3(PyNONIT)]_2$ and the monomer $[Dy(hfac)_3(H_2O)_2]$, where the symmetry of Dy^{III} ion in Dy_2O_2 decreases to D_{2d}, showing slow relaxation of the magnetization at lower temperature. Interestingly, a moisture-mediated reversible solid transformation between **1** and $([Dy(hfac)_3(H_2O)(PyNONIT)]_2)$ (**4**) has been investigated. Spongelike **1** can undergo a transition from eight to nine coordination at room temperature through hydration. A different coordination field is mostly responsible for no ac signal noticed for **4**. The structural diversity of the Dy_2 family provides an opportunity to expand the investigation on 4f single-molecule magnets. Approaches that the relaxation of the supramolecular dimer can be tuned to ON and OFF states modulated by the packing mode and ligand field are presented.
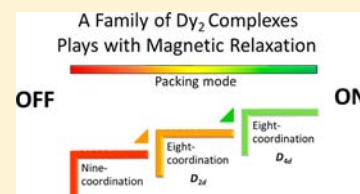
INTRODUCTION

The exploration of advanced magnetic materials has been of great interest in recent years. Since the discovery of single-molecule magnets (SMMs) with discrete molecules that exhibit slow magnetic relaxation in the low-temperature region, which expands the realization of the realms between paramagnetism and long-range ordering, this interdisciplinary field has flourished[1] with appealing phenomena and proposed applications[2] such as high-density data storage, quantum information processing systems, and spintronic devices. Of particular challenge for scientists is the increasing blocking temperature at which relaxation can occur, depending on the anisotropy barrier from a combination of the appropriate spin in the ground state and uniaxial magnetic anisotropy. It has been reported recently that comprising lanthanide ions with a large unquenched orbital momentum is a promising approach because increasing the magnetic anisotropy partially compensates for the weak exchange.[3] Among the lanthanide SMMs, dysprosium compounds are the most useful motifs for the large moment and high anisotropy of the Dy^{III} ion ($^6H_{15/2}$, $S = {}^5/_2$, $L = 5$, and $J = {}^{15}/_2$).

Chemical flexibility contributes to the variety of Dy^{III} SMMs, ranging from the mononuclear,[3a,g] binuclear,[3c,i,j] trinuclear,[3b] tetranuclear,[3d,e] and pentanuclear[3h] to Dy_{11} compounds,[3f,4] where the highest temperature of 8.3 K at which hysteresis is observed is reported by Long and co-workers in the Dy_2 compound.[3i] Retrospectively, the ligand field has been investigated deeply for its effect on the magnetic anisotropy and thus slow relaxation of the magnetization since the lanthanide single-ion magnet was found in 2003.[3a] Although this magnetic relaxation in polynuclear clusters appears to come largely from single-ion anisotropy, strong coupling through a radical bridge (with a record blocking temperature)[3i] and strong axiality and Ising exchange interaction that can suppress quantum tunneling[3j] provide strategies for enhancing the SMM properties. Especially, the exchange-blocked relaxation[5] observed recently opened up a new perspective to constructing effective SMMs. Weak exchange interactions from supramolecular hydrogen bonds in a $[Mn_4]_2$ dimer of $S = {}^9/_2$ SMMs have evidenced the tunnel resonances shifted away from zero applied field and the low probability of occurrence for a double quantum transition.[6a] These so-called exchange-biased SMMs, of which the intermolecular interactions are modulated by the terminal ligand decoration or supramolecular aggregate, present a means for fine-tuning the SMM behavior.[6]

The smaller number of Dy^{III} ions in the SMMs tends to present easier estimation and better understanding of the magnetic nature. It appears to synthesize a suitable ligand comprising an oxygen-donor atom toward lanthanide ions based on the hard−soft acid−base classification and the ability to bridge metal centers but prevent high polynuclear formation.

Table 1. Crystallographic Data and Structure Refinement for Compounds 1−4

	1	2·2CH$_2$Cl$_2$	3	4
formula	C$_{54}$H$_{38}$Dy$_2$F$_{36}$N$_6$O$_{18}$	C$_{55}$H$_{40}$Cl$_2$Dy$_2$F$_{36}$N$_6$O$_{18}$	C$_{69}$H$_{45}$Dy$_3$F$_{54}$N$_6$O$_{26}$	C$_{54}$H$_{42}$Dy$_2$F$_{36}$N$_6$O$_{20}$
M, g mol^{-1}	2067.90	2152.83	2887.61	2103.94
cryst syst	triclinic	triclinic	monoclinic	monoclinic
space group	$P\bar{1}$	$P\bar{1}$	$C2/c$	$P2_1/c$
a, Å	12.3118(9)	12.2162(6)	22.6866(6)	13.2124(5)
b, Å	13.6878(8)	12.7794(6)	13.0836(4)	24.5380(8)
c, Å	22.4436(14)	25.8325(11)	32.5926(11)	10.9894(4)
α, deg	90.813(5)	85.867(4)	90	90
β, deg	93.776(6)	88.922(4)	91.195(3)	90.840(3)
γ, deg	92.983(5)	68.762(4)	90	90
V, Å^3	3768.3(4)	3749.1(3)	9672.1(5)	3562.4(2)
Z	2	2	4	2
d_{calcd}, g cm^{-3}	1.822	1.907	1.983	1.961
temperature, K	120(2)	120(2)	120(2)	120(2)
$F(000)$	2008	2092	5572	2048
θ range, deg	2.33−25.01	2.38−25.01	2.50−25.01	2.49−25.01
completeness, %	99.9	99.8	99.9	99.9
residual map, e Å^{-3}	1.288 and −1.018	2.377 and −2.007	1.157 and −1.301	1.055 and −0.805
GOF on F^2	1.028	1.014	1.045	1.066
final indices [$I > 2\sigma(I)$]	R1 = 0.0531, wR2 = 0.1211	R1 = 0.0552, wR2 = 0.1395	R1 = 0.0509, wR2 = 0.1044	R1 = 0.0438, wR2 = 0.0771
R indices (all data)	R1 = 0.0763, wR2 = 0.1377	R1 = 0.0650, wR2 = 0.1484	R1 = 0.0751, wR2 = 0.1151	R1 = 0.0631, wR2 = 0.0834

Nitronyl nitroxides (NITs) as spin carriers are fascinating candidates for their effective exchange interactions, which have given valuable results in the field of superparamagnetic magnets.[7] In this respect, a simple oxidepyridyl group is introduced to the radical for the synthesis of binuclear lanthanide compounds. Hexafluoroacetylacetonate, a coligand, is chosen to satisfy the coordination geometry and charge balance, more importantly, to guarantee the Lewis acidity necessary for coordination of the radical.

The rational design of functional materials brings defined geometries and properties. However, the accurate self-assembly of the cystal structure is still an exciting challenge for chemists, especially in the radical-containing system. Herein, we report the syntheses, structures, and magnetic properties of four binuclear dysprosium radical compounds, {[Dy(hfac)$_3$(PyNONIT)]$_2$}$_2$ (**1**), {[Dy(hfac)$_3$(PyNONIT)]$_2$}$_2$·2CH$_2$Cl$_2$ (**2·2CH$_2$Cl$_2$**), [Dy(hfac)$_3$(PyNONIT)]$_2$[Dy$_{0.5}$(hfac)$_{1.5}$(H$_2$O)]$_2$ (**3**), and [Dy(hfac)$_3$(H$_2$O)(PyNONIT)]$_2$ (**4**), where hfac = hexafluoroacetylacetonate and PyNONIT = 2-(4-oxidopyridyl)-4,4,5,5-tetramethylimidazolin-1-oxyl-3-oxide). Double-μ_2-oxygen atoms of the N-oxide groups link metal ions to centrosymmetric bimetallic Dy$_2$O$_2$ cores in all compounds. Both the structural variety and magnetic relaxation ON or OFF of the family of Dy$_2$ are characterized and discussed. Vapor-mediated reversible transformation between **1** and **4** induced by hydation and dehydration is also investigated.

■ EXPERIMENTAL SECTION

X-ray Crystallography. Diffraction intensity data for single crystals of **1−4** were collected at 120(2) K on an Oxford Supernova diffractometer with graphite-monochromated Mo Kα radiation (λ = 0.71073 Å) using the ω-scan technique. The structures were solved by direct methods and refined by full-matrix least-squares methods on F^2 with anisotropic thermal parameters for all non-hydrogen atoms.[8] Hydrogen atoms were located geometrically and refined isotropically. Crystallographic data and structure refinement of compounds **1−4** are listed in Table 1. Selected bonds and angles are listed in the Supporting Information.

Physical Measurements. Elemental analyses for carbon, hydrogen, and nitrogen were carried out on a Perkin-Elmer analyzer. Direct-current (dc) magnetic susceptibilities were measured on a Quantum Design MPMS XL-7 SQUID magnetometer. Diamagnetic corrections were made with Pascal's constants for all of the constituent atoms and sample holders. Alternating-current (ac) magnetic susceptibility data were collected on the same instrument employing a 3.5 Oe oscillating field at frequencies up to 1200 Hz. Powder X-ray diffraction measurements were recorded on a D/Max-2500 X-ray diffractometer using Cu Kα radiation. IR spectra were recorded in the range of 400−4000 cm^{-1} on a Bruker TENOR 27 spectrophotometer using KBr pellets.

Materials. All chemicals were performed at reagent grade except that the solvents used were dried (heptane over sodium and CH$_2$Cl$_2$ over CaH$_2$) and distilled prior to use.

Synthesis of 2-(4-Oxidopyridyl)-4,4,5,5-tetramethylimidazolin-1-oxyl-3-oxide) (PyNONIT). PyNONIT was prepared by condensation of 2,3-bis(hydroxylamino)-2,3-dimethylbutane with 4-pyridinecarboxaldehyde N-oxide, followed by oxidation according to the literature method.[9]

Syntheses of 1−4. A solution of [Dy(hfac)$_3$(H$_2$O)$_2$] (0.04 mmol) in 30 mL of dry boiling heptane was heated to reflux for 1 h and then cooled to 90 °C, whereupon 6 mL of a dichloromethane solution of PyNONIT (0.036 mmol) was slowly added with stirring. The mixture was stirred for several minutes, cooled to room temperature, and left to stand in a desiccator for 48 h. Pale-green, sticklike crystals of **1** suitable for single-crystal X-ray analysis were obtained. Yield of **1**: 16% (based on ligand). Elem anal. Calcd for Dy$_2$C$_{54}$F$_{36}$O$_{18}$H$_{38}$N$_6$ (**1**): C, 31.36; H, 1.85; N, 4.06. Found: C, 31.25; H, 2.24; N, 4.02. IR (KBr): 1651(s), 1561(m), 1535(m), 1505(s), 1417(w), 1378(m), 1261(s), 1213(s), 1146(s), 1103(m), 854(w), 804(m), 661(m), 587(m) cm^{-1}. Crystals of **1** played an accompaniment to blue powders with the presence of saturated steam at room temperature for a few minutes and changed back to green powders (**1***) under a relative humidity of ~0% in a constant-temperature and -humidity box and at room temperature for hours. Elem anal. Calcd for Dy$_2$C$_{54}$F$_{36}$O$_{18}$H$_{38}$N$_6$ (**1***): C, 31.36; H, 1.85; N, 4.06. Found: C, 30.93; H, 2.19; N, 4.10.

Compound **2** was synthesized in a procedure analogous to that employed for **1**. A solution of [Dy(hfac)$_3$(H$_2$O)$_2$] (0.04 mmol) in 20 mL of dry boiling heptane was heated to reflux for 1 h and then cooled to 90 °C, whereupon 2 mL of a dichloromethane solution of PyNONIT (0.04 mmol) was slowly added with stirring. The final solution was cooled to room temperature and left to stand in a

desiccator for 48 h to give pale-green, platelike crystals. A sample maintained in contact with the mother liquor to prevent loss of the interstitial solvent was crystallographically identified as $2 \cdot 2CH_2Cl_2$. Drying under air at room temperature afforded a fully desolvated species that was analyzed as **2**. Yield of **2**: 46%. Elem anal. Calcd for $Dy_2C_{54}F_{36}O_{18}H_{38}N_6$ (**2**): C, 31.36; H, 1.85; N, 4.06. Found: C, 31.54; H, 2.26; N, 4.05. IR (KBr): 1651(s), 1561(m), 1536(m), 1504(s), 1417(w), 1378(w), 1260(s), 1216(s), 1147(s), 1103(m), 855(w), 804(m), 661(m), 588(m) cm^{-1}.

Compound **3** was also synthesized in a procedure analogous to that employed for **1**. A solution of $[Dy(hfac)_3(H_2O)_2]$ (0.06 mmol) in 30 mL of dry boiling heptane was heated to reflux for 1 h and then cooled to 90 °C, whereupon 3 mL of a dichloromethane solution of PyNONIT (0.04 mmol) was slowly added with stirring. The final solution was cooled slowly to room temperature to give blue, platelike crystals. Yield of **3**: 83%. Elem anal. Calcd for $Dy_3C_{69}F_{54}O_{26}H_{45}N_6$ (**3**): C, 28.70; H, 1.57; N, 2.91. Found: C, 28.63; H, 2.46; N, 3.13. IR (KBr): 3379(w,b), 1652(s), 1562(m), 1535(m), 1503(s), 1407(w), 1378(w), 1259(s), 1217(s), 1146(s), 1103(m), 803(m), 662(m), 588(w) cm^{-1}.

Green crystals of **1** can become blue powders and a few blue crystals suitable for single-crystal X-ray analysis with the presence of saturated steam at room temperature. Elem anal. Calcd for $Dy_2C_{54}F_{36}O_{20}H_{42}N_6$ (**4**): C, 30.83; H, 2.01; N, 3.99. Found: C, 30.59; H, 2.17; N, 3.95. IR (KBr): 3388(w,b), 1653(s), 1559(m), 1533(m), 1504(m), 1410(w), 1378(w), 1259(s), 1213(s), 1145(s), 1100(m), 850(w), 801(w), 662(m), 587(w) cm^{-1}.

■ RESULTS AND DISCUSSION

Synthesis. The Dy$_2$ families of **1**−**4** were successfully synthesized in a similar procedure using radical ligand PyNONIT with $[Dy(hfac)_3(H_2O)_2]$. A key factor in this preparation is the accurate control of moisture or water, as well as the ratio of the reactants and solvents (Scheme 1). When the

Scheme 1. Synthetic Route of the Family of Dy$_2$ Compounds
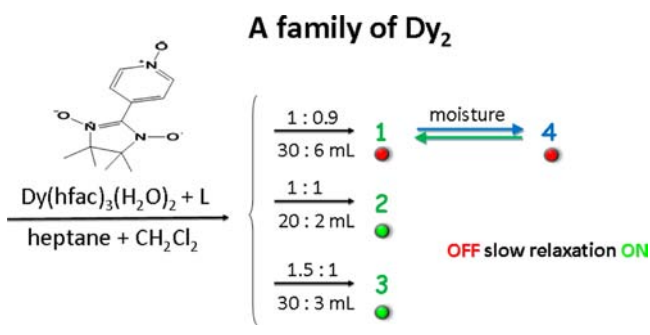

ratio of salt and radical was 1:0.9, a slow crystallization produced binuclear **1**. A rapid crystallization rate with a little more ligand (1:1) led to crystals of $2 \cdot 2CH_2Cl_2$, which could be dried under air at room temperature with loss of the interstitial solvent to a desolvated species that was analyzed as **2**. The IR spectra of compounds **1** and **2** containing the same characteristic bands present high similarity in the blocking unit of Dy$_2$ (Supporting Information, Figure S1). The reaction of salt with much less ligand (1.5:1 ≈ 1:0.7) afforded adduct **3** comprising $[Dy(hfac)_3(PyNONIT)]_2$ and additional $[Dy(hfac)_3(H_2O)_2]$. An interesting transformation between **1** and **4**, accompanied by the capture and release of water molecules with color change, has been observed. Light-green crystals of **1** became blue in the saturation water vapor at room temperature in a few minutes. The blue powder has been proven to be the same as **4** by elemental analysis and powder X-ray diffraction analysis (Supporting Information, Figure S2).

Crystal Structure Analysis. $\{[Dy(hfac)_3(PyNONIT)]_2\}_2$ (**1**) and $\{[Dy(hfac)_3(PyNONIT)]_2\}_2 \cdot 2CH_2Cl_2$ (**2·2CH$_2$Cl$_2$**). Compounds **1** and **2·2CH$_2$Cl$_2$** both crystallize in triclinic space group $P\bar{1}$ with $Z = 2$. To maintain clarity and simplicity, the solvent molecule is not considered. These two binuclear compounds differ only in the crystal packing mode, as shown in Figures 1 and 2. The structures consist of two crystallo-
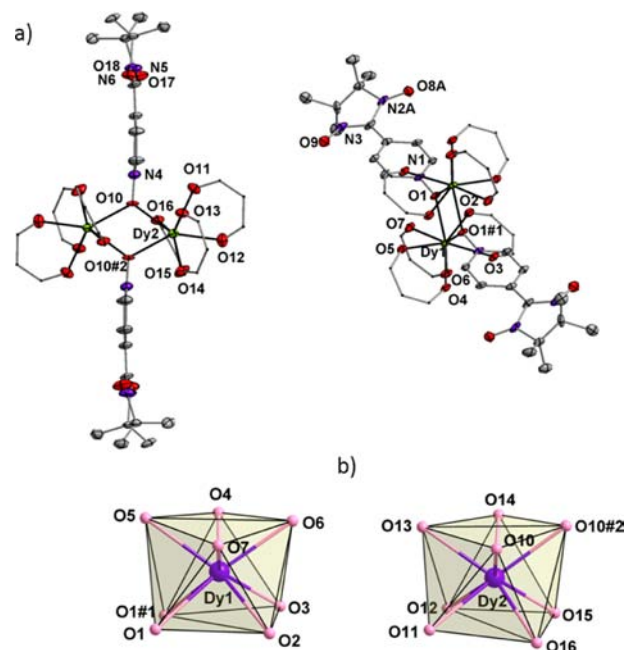
Figure 1. (a) Simplified view of the crystal structure of **1** with a labeling scheme. Thermal ellipsoids are drawn at 30% probability. Fluorine, hydrogen, and some carbon atoms are omitted for clarity. Hfac is plotted in wire style. (b) D_{4d}-symmetry polyhedra of dysprosium atoms. Symmetry code: #1, $-x + 1$, $-y$, $-z + 1$; #2, $-x$, $-y + 2$, $-z$.
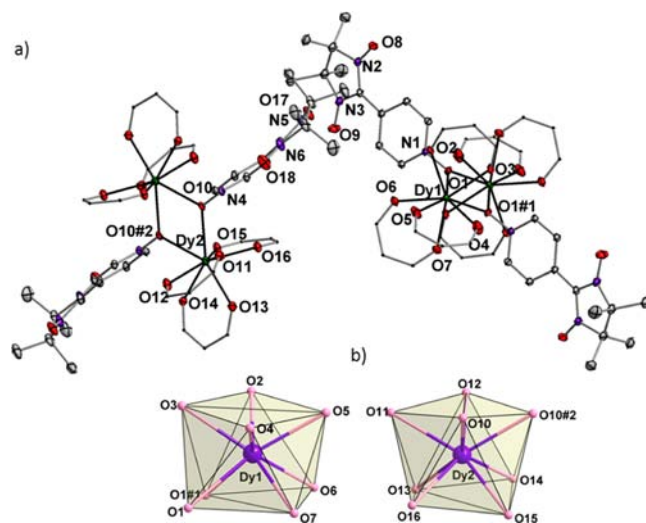
Figure 2. (a) Simplified view of the crystal structure of **2·2CH$_2$Cl$_2$** with a labeling scheme. Thermal ellipsoids are drawn at 30% probability. Fluorine, hydrogen, and some carbon atoms and solvent molecules are omitted for clarity. Hfac is plotted in wire style. (b) D_{4d}-symmetry polyhedra of dysprosium atoms. Symmetry code: #1, $-x$, $-y + 1$, $-z + 2$; #2, $-x$, $-y + 1$, $-z + 1$.

Table 2. δ and φ Values for 1 and 2·2CH$_2$Cl$_2$[a]

	1-Dy1		**1-Dy2**		**2·2CH$_2$Cl$_2$-Dy1**		**2·2CH$_2$Cl$_2$-Dy2**		**DD**	**TP**	**SAP**
δ_1	O5 [O4 O7] O6	15.222	O13 [O14 O10] O10#2	10.276(8)	O3 [O2 O4] O5	2.060	O13 [O16 O14] O15	17.972	29.5	0.0	0.0
δ_2	O1#1 [O1 O3] O2	9.250	O12 [O11 O15] O16	7.475(7)	O1#3 [O1 O6] O7	9.615	O11 [O12 O10] O10#4	11.716	29.5	21.8	0.0
δ_3	O5 [O1 O7] O2	52.149	O13 [O11 O10] O16	49.487	O3 [O1 O4] O7	46.963	O13 [O12 O14] O10#4	59.386	29.5	48.2	52.4
δ_4	O1#1 [O4 O3] O6	54.651(5)	O12 [O14 O15] O10#2	51.595	O1#3 [O2 O6] O5	51.791	O11 [O16 O10] O15	55.898	29.5	48.2	52.4
φ_1	O7−O3−O5−O1#1	32.672	O10−O15−O13−O12	22.794(4)	O4−O6−O3−O1#3	28.246	O14−O10−O13−O11	27.034	0.0	14.1	24.5
φ_2	O4−O1−O6−O2	27.741	O14−O11−O10#2−O16	30.321	O2−O1−O5−O7	21.384	O16−O12−O15−O10#4	33.346			

[a]A [B C] D is the dihedral angle between the ABC plane and the BCD plane. A−B−C−D is the dihedral angle between the (AB)CD plane and AB(CD), where (AB) signifies the midpoint of the AB edge. Symmetry code: #1, −x + 1, −y, −z + 1; #2, −x, −y + 2, −z; #3, −x, −y + 1, −z + 2; #4, −x, −y + 1, −z + 1.

graphically independent, centrosymmetric dimetallic [Dy$_2$(hfac)$_6$(PyNONIT)$_2$] units. The center ions are all surrounded with a slightly distorted square-antiprismatic DyO$_8$ coordination sphere from three bischelate hfac anions and two μ_2 bridging ligands. The Dy−O bond lengths are in the range of 2.306(6)−2.444(5) Å, where the Dy−O1 and Dy−O10 distances are longer than all of the others ascribed to the bridged character of O1 and O10 atoms (Supporting Information, Table S1). Eight-coordinate geometries are mostly taken as the D_{2d} dodecahedron (DD), C_{2v} bicapped trigonal prism (TP), and D_{4d} square antiprism (SAP). The semi-quantitative method of polytopal analysis is examined.[10] Relevant dihedral angles are summarized in Table 2. The δ_1 and δ_2 values, which represent the planarity of the squares, range from 2.06 to 17.97°. The δ_3 and δ_4 values for the triangular faces, along with the φ values, are close to the angles (52.4, 52.4, and 24.5°) of an ideal SAP polyhedron, respectively, indicative of D_{4d} symmetry. A continuous symmetry measurement method is performed to further evaluate the polyhedral shape of the metal coordination sphere. The shape values of less than 1.0 with SAP ensure D_{4d} site symmetry (Table 3).[11] The Dy$_2$O$_2$ cores appear to be

Table 3. Lanthanide Geometry Analysis by SHAPE Software

Dy^{III}	D_{2d} DD	C_{2v} TP	D_{4d} SAP
1-Dy1	1.341	1.876	0.651
1-Dy2	1.375	2.011	0.671
2·2CH$_2$Cl$_2$-Dy1	1.678	2.171	0.768
2·2CH$_2$Cl$_2$-Dy2	1.020	2.078	0.967
3-Dy1	0.743	1.803	2.295
3-Dy2	0.303	2.422	2.627

approximately rhombic bridged by *N*-oxide groups of ligands. Dy···Dy distances and Dy−O−Dy angles for **1** and **2·2CH$_2$Cl$_2$** that confirm the centrosymmetric binuclear Dy$_2$O$_2$ are 4.06 Å and 116.3° with very little up-and-down motion, respectively (Table 4). An inspection of the intermolecular interactions results in the nearest Dy···Dy distances of 9.9749(8) and

8.7640(7) Å for **1** and **2·2CH$_2$Cl$_2$**, respectively. Weak intermolecular hydrogen bonds for **1** are of C$_{12B}$−H$_{12E}$···O$_{17}$, C$_{19}$−H$_{19}$···F$_{25A}$, and C$_{38}$−H$_{38B}$···F$_{33}$ with H···O distances of 2.45, 2.48, and 2.49 Å and C−H···O angles of 121, 152, and 156°, respectively (Supporting Information, Figure S3). The O···O separation between the uncoordinated NIT groups is 4.8276(3) Å, that as far as the interactions are concerned, can be neglected. The Dy$_2$ cores in **2·2CH$_2$Cl$_2$** are also linked to the 3D network by C−H···O and C−H···F hydrogen bonds (Supporting Information, Figure S4), as well as the O···O separation between the uncoordinated NIT groups with 3.2418(113) Å.

[Dy(hfac)$_3$(PyNONIT)]$_2$[Dy$_{0.5}$(hfac)$_{1.5}$(H$_2$O)]$_2$ (3). 3 crystallizes in monoclinic space group C2/c. As shown in Figure 3,
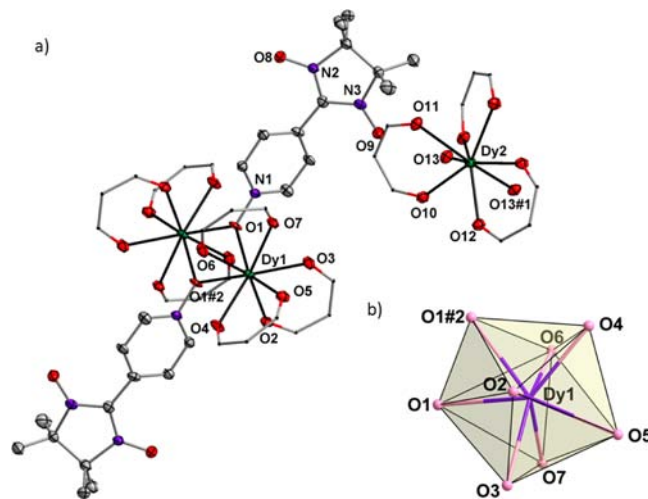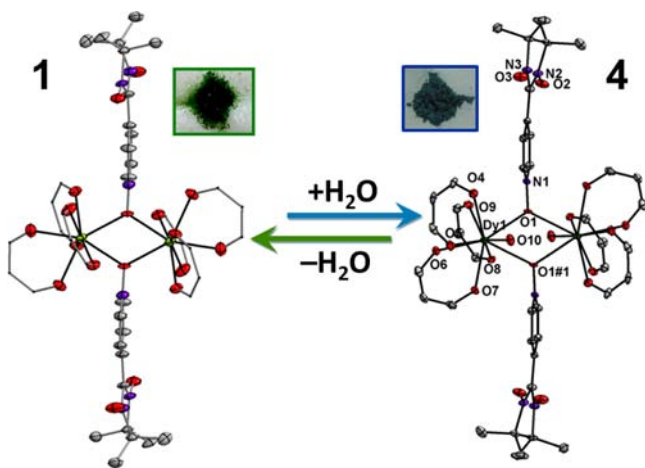

Figure 3. Simplified view of the crystal structure of **3** with a labeling scheme. Thermal ellipsoids are drawn at 30% probability. Fluorine, hydrogen, and some carbon atoms are omitted for clarity. Hfac is plotted in wire style. (b) D_{2d}-symmetry polyhedron of the dysprosium atom. Symmetry code: #1, −x − 1, y, −z − $^1/_2$; #2, −x − $^1/_2$, −y + $^1/_2$, −z.

Table 4. Dy···Dy Distances and Dy−O−Dy Angles in the Dy$_2$O$_2$ Cores for 1 and 2·2CH$_2$Cl$_2$

	1-Dy1	**1-Dy2**	**2·2CH$_2$Cl$_2$-Dy1**	**2·2CH$_2$Cl$_2$-Dy2**
Dy···Dy/Å	4.0763(5)	4.0368(6)	4.0868(6)	4.1039(5)
Dy−O−Dy/deg	116.395(180)	115.497(174)	116.182(195)	116.968(205)

there are two independent dysprosium ions in the least repeated unit. Dy1 locates in an eight-coordinated geometry completed by three bichelated hfac anions and two μ_2 bridging ligands. A centrosymmetric binuclear Dy$_2$ is thus formed with a distorted DD oxygenated coordination sphere, where Dy–O bonds range from 2.312(5) to 2.412(5) Å (Supporting Information, Table S2). Characteristic angle values calculated for a polyhedron of Dy1 are 20.26, 35.35, 39.03, 30.39, 6.64, and 5.97°, and the local symmetry is nearly D_{2d}, in comparison with D_{4d} in 1 and 2·2CH$_2$Cl$_2$ (Supporting Information, Table S3). Double-μ_2-oxygen-bridged Dy$_2$O$_2$ shows a Dy···Dy distance of 4.0930(6) Å and a Dy–O–Dy angle of 117.126(210)°, respectively. Dy2 is coordinated by eight oxygen atoms, in which six oxygen atoms are from three hfac anions and two oxygen atoms are from coordinated water molecules with Dy–O bonds of 2.300(5)–2.403(5) Å, forming a centrosymmetric mononuclear [Dy(hfac)$_3$(H$_2$O)$_2$] complex. In addition, the shape measurements assume a triangle DD with D_{2d} for both dimer and monomer (Table 3). Hydrogen bonds combine the isolated binuclear and mononuclear complexes into the 3D framework with H···O distances of 1.97 and 1.98 Å and O–H···O angles of 146 and 135°, involving the acceptor oxygen atoms from the NIT moiety and the donor hydrogen atoms from coordinated water molecules (Supporting Information, Figure S5). The nearest O···O distance between the uncoordinated NIT groups is 4.1347(74) Å.

[Dy(hfac)$_3$(H$_2$O)(PyNONIT)]$_2$ (4). 4 crystallizes in monoclinic space group $P2_1/c$ with $Z = 2$. The asymmetric unit is made of one crystallographically independent, centrosymmetric binuclear unit (Figure 4). The Dy^{III} ion is nine-coordinated,


Figure 4. Reversible transformation between 1 and 4 accompanied by the capture and release of water molecules, as well as a simplified view of the crystal structure of 4 with a labeling scheme. Thermal ellipsoids are drawn at 30% probability. Fluorine, hydrogen, and some carbon atoms are omitted for clarity. Symmetry code: #1, −x, −y − 1, −z.

surrounded by oxygen atoms, six of which are from the hfac groups, two from the μ_2 bridging ligands, and one from a coordinated water molecule. The binuclear dysprosium core is bridged by the N-oxide moiety from two ligands with a Dy···Dy distance and a Dy–O–Dy angle of 4.2702(4) Å and 119.868(150)°, respectively. An intramolecular hydrogen bond is formed between the hydrogen atom of a coordinated water molecule and the oxygen atom of a hfac anion with a H···O (C$_{10}$–H$_{10D}$···O$_8$) distance of 2.13 Å. Compound 4 is obtained by hydration of 1, as referred to previously. Moreover,

if exposed to a relative humidity of ∼0% in a constant-temperature and -humidity box and at room temperature for several hours, the light green of 1 would be recovered (1*; Supporting Information, Figure S2), indicating that the Dy^{III} coordination could undergo reversible change by controlling the water molecule.

**Magnetic Properties.** *1 and 2.* The dc magnetic susceptibility data of 1 and 2 are shown in Figure 5. At 300
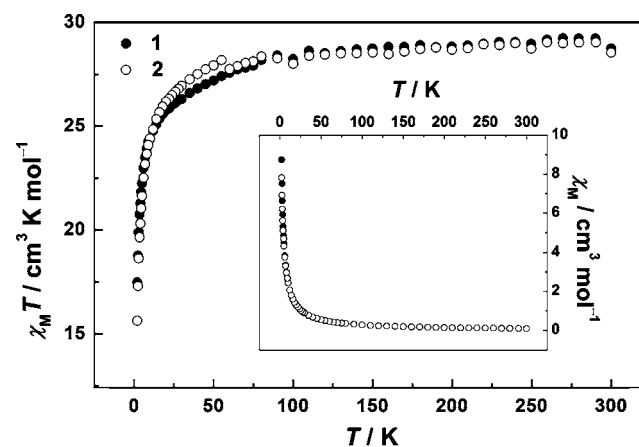
Figure 5. Temperature dependence of $\chi_M T$ for compounds 1 and 2. Inset: temperature dependence of χ_M for 1 and 2.

K, the $\chi_M T$ values are 28.74 and 28.55 cm^3 K mol^{-1} for 1 and 2, respectively, slightly lower than the expected value of 29.09 cm^3 K mol^{-1} for two isolated Dy^{III} ions (^{6}H$_{15/2}$) plus two radicals ($S = 1/2$). As the temperature is lowered, the $\chi_M T$ values decrease gradually and more dramatically below 60 K to the minima of 17.49 and 15.63 cm^3 K mol^{-1} at 2 K for 1 and 2, respectively. Fitting the data in the range of 2−300 K with the Curie−Weiss law [$\chi_M = C/(T-\theta)$] gives the results of $C = 29.30$ cm^3 mol^{-1} K and $\theta = -2.62$ K for 1 and $C = 29.09$ cm^3 mol^{-1} K and $\theta = -2.19$ K for 2, respectively. The negative θ values and a decrease of the $\chi_M T$ values could be ascribed to thermal depopulation of the Stark levels of the Dy^{III} ions and/or the possible antiferromagnetic interactions between the spin carriers.

The interactions between dysprosium ions can be simulated in a very low-temperature region with an effective spin $S = 1/2$ and anisotropic g tensor.[12] When only the z components are considered in the zero-field limit, the expression for the temperature dependence of magnetic susceptibilities is $\chi_M T = (Ng^2\beta/3k)/[1 + \exp(-J/2kT)]$.[13] The best fit with the dimer Ising model in the temperature range between 1 and 9 K yields $J = -2.0$ cm^{-1} and $g = 20.4$ for 1 and $J = -2.5$ cm^{-1} and $g = 20.6$ for 2, respectively (Figure 6). The field dependence of the magnetization for the two compounds at 2.0 K, mapped in Figure S6 in the Supporting Information, reveals that the corresponding highest M values are 14.97 and 14.36 $N\beta$ at 50 kOe, respectively. When $S = 1/2$ and $g \approx 20$ are taken, a lack of saturation of magnetization can be found due to the presence of large magnetic anisotropy and/or low-lying excited states, as well as proven by nonsuperposition on $M/N\beta$ versus HT^{-1} at various magnetic fields (Supporting Information, Figure S7). Inspection on the hysteresis loop exhibits a small coercive field at 2 K for 2.

Exploration of the dynamic magnetic properties should be another important characterization for Dy$_2$O$_2$ compounds,
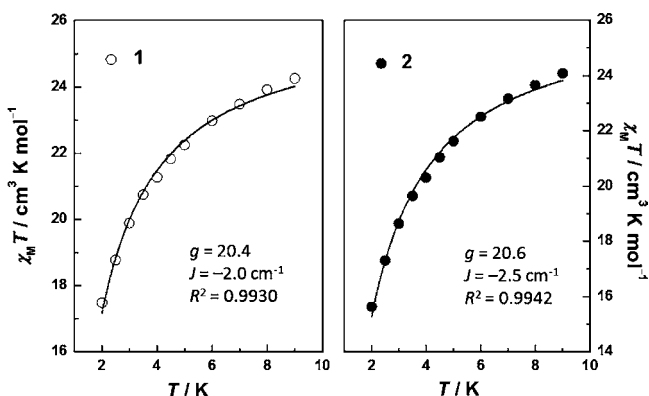
Figure 6. Temperature dependence of $\chi_M T$ for compounds **1** and **2** in the range of 1−9 K with the best fit using the dimer Ising model.

although a high similarity is found in static magnetic measurements. The out-of-phase component of the ac susceptibility for **1** does not exhibit any visible peak upon 2 K in the absence of a dc field. Compound **2** shows, however, significant frequency-dependent in-phase and out-of-phase signals, suggesting slow relaxation of the magnetization in **2** at low temperature (Figure 7). Unfortunately, the energy
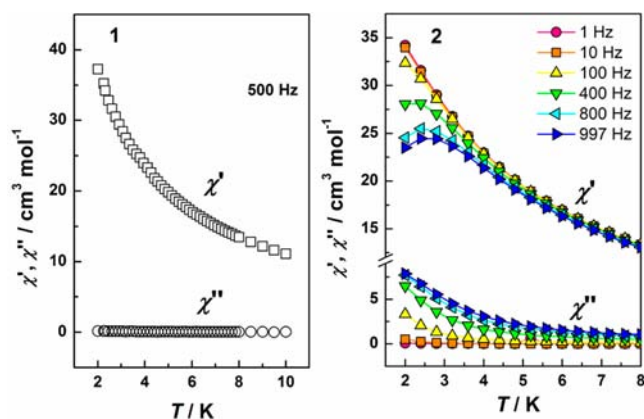
Figure 7. Temperature dependence of the imaginary χ'' and real χ' components of the ac susceptibility measured in zero applied field for **1** and **2**. The lines are guides for the eyes.

barrier cannot be extracted from this set of data because no maximum of χ'' is observed in the temperature window technically available. Alternatively, an equation $\ln(\chi''/\chi') = \ln(\omega\tau_0) + E_a/k_B T$ has been employed to evaluate the energy barrier and prefactor roughly with the assumption that there is only one characteristic relaxation process.[14] Appling this method by fitting the experimental data results in an estimation of the activation energy of ~5 K and τ_0 of 10^{-5} s (Supporting Information, Figure S8).

3. The $\chi_M T$ measurement performed on **3** gives the value of 21.51 cm³ K mol⁻¹ at room temperature, close to the expected value of 21.63 cm³ K mol⁻¹ (one and a half isolated Dy^III ions and one radical). The $\chi_M T$ values decrease gradually upon cooling to ca. 60 K and then quickly down to 12.86 cm³ K mol⁻¹ at 2 K, as shown in Figure 8. The data in the range of 2−300 K obey the Curie−Weiss law with C = 22.07 cm³ mol⁻¹ K and θ = −2.85 K, corresponding to a combination of possible antiferromagnetic interaction and thermal depopulation of low-lying crystal-field states. The magnetization increases upon
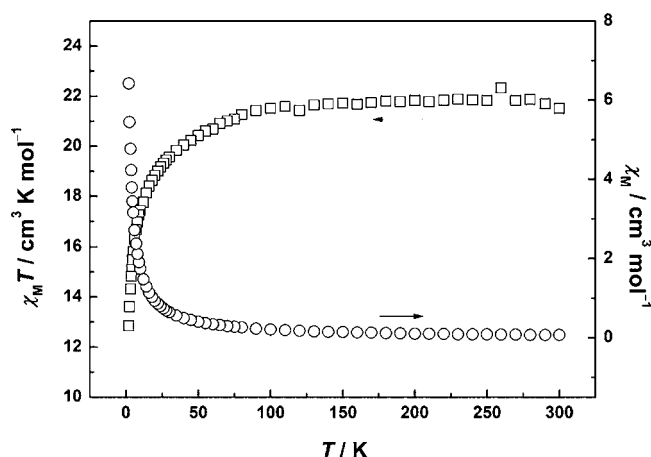
Figure 8. Temperature dependence of χ_M and $\chi_M T$ for compound **3**.

exposure to an external field but cannot be saturated at 70 kOe, which may result from large magnetic anisotropy and/or the lack of a well-defined ground state, as also proven by nonsuperposition on $M/N\beta$ versus HT^{-1} data (Supporting Information, Figures S9 and S10). The ac magnetic measurement shows a frequency dependence of magnetic susceptibilities in an out-of-phase signal, indicating slow relaxation of the magnetization (Figure 9). However, no peaks can be obtained,
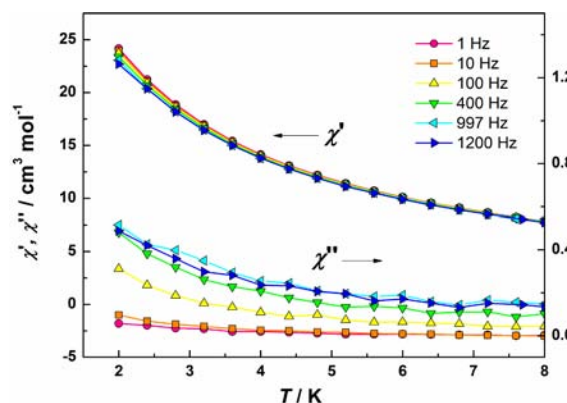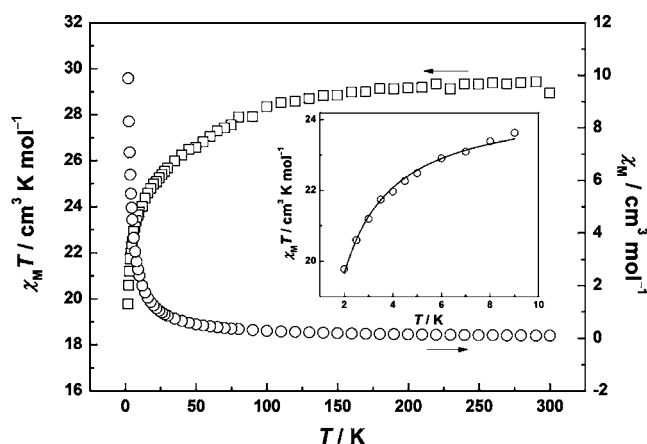

Figure 9. Temperature dependence of the imaginary χ'' and real χ' components of the ac susceptibility measured in zero applied field for **3**. The lines are guides for the eyes.

possibly because of general quantum tunneling. The estimated E_a/k_B and τ_0 values from the linear plots are $E_a/k_B \approx 2$ K and τ_0 of 10^{-5} s (Supporting Information, Figure S11).

4. The dc magnetic susceptibility data for **4** are shown in Figure 10. The $\chi_M T$ value of 28.94 cm³ K mol⁻¹ at 300 K is well consistent with the expected value of 29.09 cm³ K mol⁻¹ for two free Dy^III ions with two radicals. Upon cooling, the $\chi_M T$ product decreases slowly until ~100 K and then dramatically to a minimum of 19.77 cm³ K mol⁻¹ at 2 K. The best fit with the dimer Ising model in the temperature range of 1−9 K is found for J = −1.1 cm⁻¹ and g = 19.8. The field dependence of the magnetization at 2 K shows that the magnetization increases up to 14.37 $N\beta$ at 70 kOe but does not reach the expected saturation value (Supporting Information, Figure S12). No out-of-phase ac signal is noticed above 2 K for **4** (Supporting Information, Figure S13).

Dimetallic Dy_2O_2 bridged by double-μ_2-oxygen atoms of the N-oxide groups is realized in the metal−radical approach for

Figure 10. Temperature dependence of χ_M and $\chi_M T$ for **4**. Inset: best fit with a dimer Ising model in the range of 1–9 K.

the first time. Moreover, a series of binuclear molecules employing this bridged mode have been characterized crystallographically and magnetically. As is evidenced in Figure 7, compounds **1** and **2** show distinctly different ac magnetism, even though they contain the same building block; that is, the local environment on the dyprosium ion and parameters of binuclear Dy_2O_2 are nearly identical, and thus the dc magnetic properties are highly similar. Therefore, the mostly resonable explanation is that quantum tunneling can be suppressed for intermolecular interactions,[6] in accordance with stronger J values obtained ($J = -2.0$ cm^{-1} for **1** and -2.5 cm^{-1} for **2**), which makes the blocking temperature move to the high-temperature region, although the origin of this is uncertain and difficult to ascertain in the absence of a crystal structure for desolvated **2**. Recently, a similar Dy^{III}-based dimer with the formula $[Dy(hfac)_3(PyNO)]_2$ (PyNO = pyridine-N-oxide) has been reported.[15] A double-μ_2-oxygen mode links two dysprosium atoms to form a centrosymmetric dimer with D_{4d} site symmetry and shows remarkable SMM behavior with extracted relaxation times in a zero static magnetic field. It could be concluded that the free NO groups from the NIT moiety can have an important impact on the slow magnetization reversal including electronic effects and dipolar interactions.

Compound **3** consists of two relatively isolated components, binuclear and mononuclear units. Significantly, the symmetry of the dysprosium atom in Dy_2O_2 decreases from D_{4d} to D_{2d}, accompanied by a weaker ac signal and a lower blocking temperature (peak values can be obtained from the temperature dependence of the real components at high frequencies for **2**, not for **3**), considering the nonnegligible effect of the monomer. This behavior could be understood as high-symmetry environments around the Dy^{III} ion favoring high blocking temperature.[3a,g,16]

Spongelike **1** can undergo transformation between eight- and nine-coordination at room temperature through hydration and dehydration. The Dy^{III} ion in compound **4** with a nine-coordinated DyO_9 coordination environment is also linked to the other Dy^{III} ion via double-μ_2-oxygen bridges with similar Dy···Dy distance and Dy–O–Dy angle. The different symmetry and strength of the local coordination field, which may strongly affect the magnetic anisotropy, are mostly responsible for no ac signal observed above 2 K.

All in all, whether the magnetic relaxation is ON or OFF in the Dy_2O_2 radical system depends on the factors of intermolecular interactions and local coordination field, highlighting the opportunity to tune the magnetic properties.

CONCLUSIONS

In summary, we have reported a family of binuclear $Dy_2(\mu_2\text{-}O)_2$ compounds based on the NIT radical. The centrosymmetric dimers bridged by NO groups play with the magnetic relaxation ON and OFF. On the one hand, intermolecular interactions can modulate the relaxation, as observed in **1** and **2**. On the other hand, the local symmetry of the center ions, as well as the coordination number could modify the character of the magnetic relaxation. Interestingly, the reversible vapor-mediated transformation performs on the eight- and nine-coordinated compounds. We emphasize the possibility of designing better SMMs if some appropriate chemical modifications are made.

ASSOCIATED CONTENT

ⓈSupporting Information

CIF files, additional structural plots and tables, additional magnetic data, IR spectra, and X-ray diffraction patterns. This material is available free of charge via the Internet at http://pubs.acs.org.

AUTHOR INFORMATION

Corresponding Author

*E-mail: shiwei@nankai.edu.cn (W.S.), pcheng@nankai.edu.cn (P.C.). Fax: (+86)22-23502458.

Notes

The authors declare no competing financial interest.

ACKNOWLEDGMENTS

REFERENCES

(1) (a) Gatteschi, D.; Sessoli, R.; Villain, J. *Molecular Nanomagnets*; Oxford University Press: London, 2006. (b) Sessoli, R.; Gatteschi, D.; Caneschi, A.; Novak, M. A. *Nature* **1993**, *365*, 141.

(2) (a) Thomas, L.; Lionti, F.; Ballou, R.; Gatteschi, D.; Sessoli, R.; Barbara, B. *Nature* **1996**, *383*, 145. (b) Jones, J. A. *Science* **1998**, *280*, 229. (c) Bogani, L.; Wernsdorfer, W. *Nat. Mater.* **2008**, *7*, 179. (d) Mannini, M.; Pineider, F.; Danieli, C.; Totti, F.; Sorace, L.; Sainctavit, Ph.; Arrio, M.-A.; Otero, E.; Joly, L.; Cezar, J. C.; Cornia, A.; Sessoli, R. *Nature* **2010**, *468*, 417.

(3) (a) Ishikawa, N.; Sugita, M.; Ishikawa, T.; Koshihara, S.-Y.; Kaizu, Y. *J. Am. Chem. Soc.* **2003**, *125*, 8694. (b) Tang, J.-K.; Hewitt, I.; Madhu, N. T.; Chastanet, G.; Wernsdorfer, W.; Anson, C. E.; Benelli, C.; Sessoli, R.; Powell, A. K. *Angew. Chem., Int. Ed.* **2006**, *45*, 1729. (c) Lin, P. H.; Burchell, T. J.; Clérac, R.; Murugesu, M. *Angew. Chem., Int. Ed.* **2008**, *47*, 8848. (d) Lin, P. H.; Burchell, T. J.; Ungur, L.; Chibotaru, L. F.; Wernsdorfer, W.; Murugesu, M. *Angew. Chem., Int. Ed.* **2009**, *48*, 9489. (e) Guo, Y. N.; Xu, G. F.; Gamez, P.; Zhao, L.; Lin, S. Y.; Deng, R.; Tang, J.; Zhang, H. J. *J. Am. Chem. Soc.* **2010**, *132*, 8538. (f) Hewitt, I. J.; Tang, J.; Madhu, N. T.; Anson, C. E.; Lan, Y.-H.; Luzon, J.; Etienne, M.; Sessoli, R.; Powell, A. K. *Angew. Chem., Int. Ed.* **2010**, *49*, 6352. (g) Jiang, S. D.; Wang, B. W.; Su, G.; Wang, Z. M.; Gao, S. *Angew. Chem., Int. Ed.* **2010**, *49*, 7448. (h) Blagg, R. J.; Muryn, C. A.; McInnes, E. J. L.; Tuna, F.; Winpenny, R. E. P. *Angew. Chem., Int. Ed.* **2011**, *50*, 6530. (i) Rinehart, J. D.; Fang, M.; Evans, W. J.; Long, J. R. *Nat. Chem.* **2011**, *3*, 538. (j) Guo, Y. N.; Xu, G. F.;

Wernsdorfer, W.; Ungur, L.; Guo, Y.; Tang, J.; Zhang, H. J.; Chibotaru, L. F.; Powell, A. K. *J. Am. Chem. Soc.* **2011**, *133*, 11948. (k) Rinehart, J. D.; Fang, M.; Evans, W. J.; Long, J. R. *J. Am. Chem. Soc.* **2011**, *133*, 14236.

(4) (a) Tian, H.-Q.; Guo, Y.-N.; Zhao, L.; Tang, J.-K.; Liu, Z.-L. *Inorg. Chem.* **2011**, *50*, 8688. (b) Canaj, A. B.; Tzimopoulos, D. I.; Philippidis, A.; Kostakis, G. E.; Milios, C. J. *Inorg. Chem.* **2012**, *51*, 7451. (c) Guo, Y.-N.; Chen, X.-H.; Xue, S.-F.; Tang, J.-K. *Inorg. Chem.* **2012**, *51*, 4035. (d) Alexandropoulos, D. I.; Mukherjee, S.; Papatriantafyllopoulou, C.; Raptopoulou, C. P.; Psycharis, V.; Bekiari, V.; Christou, G.; Stamatatos, T. C. *Inorg. Chem.* **2011**, *50*, 11276. (e) Ke, H.-S.; Xu, G.-F.; Zhao, L.; Tang, J.-K.; Zhang, X.-Y.; Zhang, H.-J. *Chem.—Eur. J.* **2009**, *15*, 10335. (f) Miao, Y.-L.; Liu, J.-L.; Li, J.-Y.; Leng, J.-D.; Ou, Y.-C.; Tong, M.-L. *Dalton Trans.* **2011**, *40*, 10229.

(5) Mondal, K. C.; Sundt, A.; Lan, Y.-H.; Kostakis, G. E.; Waldmann, O.; Ungur, L.; Chibotaru, L. F.; Anson, C. E.; Powell, A. K. *Angew. Chem., Int. Ed.* **2012**, *51*, 7550.

(6) (a) Wernsdorfer, W.; Aliaga-Alcalde, N.; Hendrickson, D. N.; Christou, G. *Nature* **2002**, *416*, 406. (b) Boskovic, C.; Bircher, R.; Tregenna-Piggott, P. L. W.; Güdel, H. U.; Paulsen, C.; Wernsdorfer, W.; Barra, A.-L.; Khatsko, E.; Neels, A.; Stoeckli-Evans, H. *J. Am. Chem. Soc.* **2003**, *125*, 14046. (c) Bagai, R.; Wernsdorfer, W.; Abboud, K. A.; Christou, G. *J. Am. Chem. Soc.* **2007**, *129*, 12918. (d) Das, A.; Gieb, K.; Krupskaya, Y.; Demeshko, S.; Dechert, S.; Klingeler, R.; Kataev, V.; Büchner, B.; Müller, P.; Meyer, F. *J. Am. Chem. Soc.* **2011**, *133*, 3433. (e) Nguyen, T. N.; Wernsdofer, W.; Abboud, K. A.; Christou, G. *J. Am. Chem. Soc.* **2011**, *133*, 20688. (f) Long, J.; Habib, F.; Lin, P.-H.; Korobkov, I.; Enright, G.; Ungur, L.; Wernsdorfer, W.; Chibotaru, L. F.; Murugesu, M. *J. Am. Chem. Soc.* **2011**, *133*, 5319.

(7) (a) Caneschi, A.; Gatteschi, D.; Lalioti, N.; Sangregorio, C.; Sessoli, R.; Venturi, G.; Vindigni, A.; Rettori, A.; Pini, M. G.; Novak, M. A. *Angew. Chem., Int. Ed.* **2001**, *40*, 1760. (b) Bogani, L.; Sangregorio, C.; Sessoli, R.; Gatteschi, D. *Angew. Chem., Int. Ed.* **2005**, *44*, 5817. (c) Bernot, K.; Bogani, L.; Caneschi, A.; Gatteschi, D.; Sessoli, R. *J. Am. Chem. Soc.* **2006**, *128*, 7947. (d) Bernot, K.; Bogani, L.; Sessoli, R.; Gatteschi, D. *Inorg. Chim. Acta* **2007**, *360*, 3807. (e) Ishii, N.; Okamura, Y.; Chiba, S.; Nogami, T.; Ishida, T. *J. Am. Chem. Soc.* **2008**, *130*, 24. (f) Poneti, G.; Bernot, K.; Bogani, L.; Caneschi, A.; Sessoli, R.; Wernsdorfer, W.; Gatteschi, D. *Chem. Commun.* **2007**, 1807. (g) Liu, R.-N.; Li, L.-C.; Wang, X.-L.; Yang, P.-P.; Wang, C.; Liao, D.-Z.; Sutter, J.-P. *Chem. Commun.* **2010**, *46*, 2566. (h) Wang, X.-L.; Li, L.-C.; Liao, D.-Z. *Inorg. Chem.* **2010**, *49*, 4735. (i) Bernot, K.; Pointillart, F.; Rosa, P.; Etienne, M.; Sessoli, R.; Gatteschi, D. *Chem. Commun.* **2010**, *46*, 6458.

(8) Sheldrick, G. *Acta Crystallogr.* **2008**, *A64*, 112.

(9) Ullman, E. F.; Osiecki, J. H.; Boocock, D. G. B.; Darcy, R. *J. Am. Chem. Soc.* **1972**, *94*, 7049.

(10) (a) Muetterties, E. L.; Guggenberger, L. J. *J. Am. Chem. Soc.* **1974**, *96*, 1748. (b) Drew, M. G. B. *Coord. Chem. Rev.* **1977**, *24*, 179.

(11) (a) Zabrodsky, H.; Peleg, S.; Avnir, D. *J. Am. Chem. Soc.* **1992**, *114*, 7843. (b) Pinsky, M.; Avnir, D. *Inorg. Chem.* **1998**, *37*, 5575.

(12) Sessoli, R.; Powell, A. K. *Coord. Chem. Rev.* **2009**, *253*, 2328.

(13) Pointillart, F.; Gal, Y. L.; Golhen, S.; Cador, O.; Ouahab, L. *Chem.—Eur. J.* **2011**, *17*, 10397.

(14) Bartolome, J.; Filoti, G.; Kuncser, V.; Schinteie, G.; Mereacre, V.; Anson, C. E.; Powell, A. K.; Prodius, D.; Turta, C. *Phys. Rev. B* **2009**, *80*, 014430.

(15) Yi, X.-H.; Bernot, K.; Pointillart, F.; Poneti, G.; Calvez, G.; Daiguebonne, C.; Guillou, O.; Sessoli, R. *Chem.—Eur. J.* **2012**, *18*, 11379.

(16) (a) Ishikawa, N.; Sugita, M.; Wernsdorfer, W. *Angew. Chem., Int. Ed.* **2005**, *44*, 2931. (b) AlDamen, M. A.; Clemente-Juan, J. M.; Coronado, E.; Marti-Gastaldo, C.; Gaita-Arino, A. *J. Am. Chem. Soc.* **2008**, *130*, 8874.